Received: 4 April 2024 | Revised: 14 August 2024 | Accepted: 17 September 2024

DOI: 10.1002/met.70004

RESEARCH ARTICLE

Meteorological Applications
Science and Technology for Weather and Climate
Open Access
RMetS

An asymmetric tropical cyclone rainfall model in the Northern Vietnam coast

Warinthorn Angkanasirikul[1] | **Wei Jian**[2] | **Edmond Yat-Man Lo**[1,2]

[1]Institute of Catastrophe Risk Management, Nanyang Technological University, Singapore, Singapore

[2]School of Civil and Environmental Engineering, Nanyang Technological University, Singapore, Singapore

Correspondence
Warinthorn Angkanasirikul, Institute of Catastrophe Risk Management, Nanyang Technological University, Singapore, Singapore.
Email: angk0063@e.ntu.edu.sg

Funding information
Nanyang Technological University

Abstract

Rainfall associated with landfalling tropical cyclones (TCs) along the Northern Vietnam coast is examined to develop an asymmetric parametric TC-induced rainfall model starting from the axisymmetric Rain-Climatology and Persistence (R-CLIPER) model. We recalibrated the R-CLIPER model (original R-CLIPER denoted as NHC) against observed rainfall patterns of 14 landfalling TCs from 2001 to 2021 in the Northern Vietnam coast, while relaxing the model's underlying linear relationships. The recalibrated R-CLIPER (denoted as Fit-Ax), still axisymmetric, suggests that some parameters are better correlated with the normalized maximum wind speed using logarithmic and exponential relationships. Fit-Ax reduces the 12-hr total rainfall overall root-mean-square errors (RMSEs) and Bias magnitudes in the before- and after-landfall periods from NHC for the entire 500-km TC domain. We further redistribute the Fit-Ax rainfall intensity across the four quadrants with respect to the TC forward motion to account for the observed large asymmetry in quadrant rainfall (version denoted as Fit-As). The vertical wind shear (VWS) and landfall (before or after) are considered in this redistribution. Fit-As generally outperforms Fit-Ax and NHC in reproducing the observed rainfall distribution for the 14 TCs. At the quadrant level, both Fit-Ax and Fit-As show significant improvement in Bias over NHC. Fit-As is further better overall in RMSE and Skill when weighted by quadrant rainfall volume. In pattern matching, Fit-As produces the best grid-averaged Pearson correlation coefficients for 11 TCs. In addition, its equitable threat scores (ETSs) are best beyond the 20-mm rainfall threshold, with the maximum of 0.299 at the 90-mm rainfall threshold. Thus, our locally fitted asymmetric rainfall model demonstrates improved capability in reproducing the historical TC-induced rainfall along the Northern Vietnam coast.

KEYWORDS

landfalling tropical cyclones, parametric rainfall model, quadrant asymmetry, tropical cyclone rainfall

1 | INTRODUCTION

Northern Vietnam (Figure 1) is one of the densely populated regions in Vietnam, with the majority of the population living in urban areas, and particularly Hanoi, the capital city (Nguyen Van et al., 2022). The Red River Delta within this region, known for its agriculture, fisheries, and manufacturing industries, is one of the most economically developed areas in Vietnam (Wells et al., 2005). However, it is also geographically vulnerable to tropical cyclones (TCs) impacts, given that the Western North Pacific (WNP) basin is frequented by intense TCs (Wang et al., 2017). On average, Northern Vietnam experiences approximately six to eight TCs annually (ISPONRE, 2009), with most of these storms occurring between July and November during the rainy season (Huang et al., 2017). For instance, Northern Vietnam experienced two major TCs in 2014: Typhoon (TY) Rammasun in July and TY Kalmaegi in September. Both resulted in extreme rainfall, strong winds, and extensive floods to the region (Davies, 2014; ESCAP/WMO Typhoon Committee, 2014). In particular, TY Rammasun impacted more than 10 million people and caused economic loss of around $50 billion USD (Mühr et al., 2014). These events highlight the potential of disastrous impact from landfalling TCs in the region, and the importance of having proper hazard assessment tools.

Rodgers et al. (2000) indicates that the TC-induced rainfall accounted for around 12% of the total rainfall impacting the WNP basin from June to November. Pham-Thanh et al. (2020) investigated spatial patterns of the rainfall and its associations with TCs over 130 meteorological stations from 1979 to 2019 in Vietnam. They reported that the radial distance for rainfall under the influence of TCs is up to 500 km from TC centers. Numerical modelling of TC-induced rainfall forecast has been carried out for the region. For example, Hung et al. (2023) investigated quantitative precipitation forecasts of TC landfalls on Vietnam's coast by integrating Short-Range Warning of Intense Rainstorms in Localized Systems (SWIRLS) with the WRF-ARW model for predicting rainfall up to 250 km radially from TC center. However, such numerical modellings often require integrating and solving model equations on high-resolution grids, and thus can be computationally intense. Besides numerical models, parametric TC-induced rainfall models have been developed linking rainfall intensity with TC intensity for operational purposes. These empirical models are fitted using the characteristics of historical TCs and the associated TC rainfall to estimate the amount of rainfall given a TC scenario. They serve as fast and valuable tools for assessing the potential rainfall impact of TCs, assisting the decision-making and disaster preparedness efforts.

At least four open-source parametric TC rainfall models are reported for operational purposes, namely, R-CLIPER (Rain-Climatology and Persistance) (Lonfat et al., 2004; Marks & DeMaria, 2003), IPET (Interagency Performance Evaluation Task Force Rainfall Analysis) (IPET, 2006), PHRaM (Parametric Hurricane Rainfall Model) (Lonfat et al., 2007), and P-CLIPER (PDF Precipitation-Climatology and Persistance) (Geoghegan et al., 2018). R-CLIPER and P-CLIPER estimate axisymmetric rainfall profiles, while IPET and PHRaM consider asymmetry. Brackins and Kalyanapu (2020) evaluated these four models for 67 Atlantic TCs between 2004 and

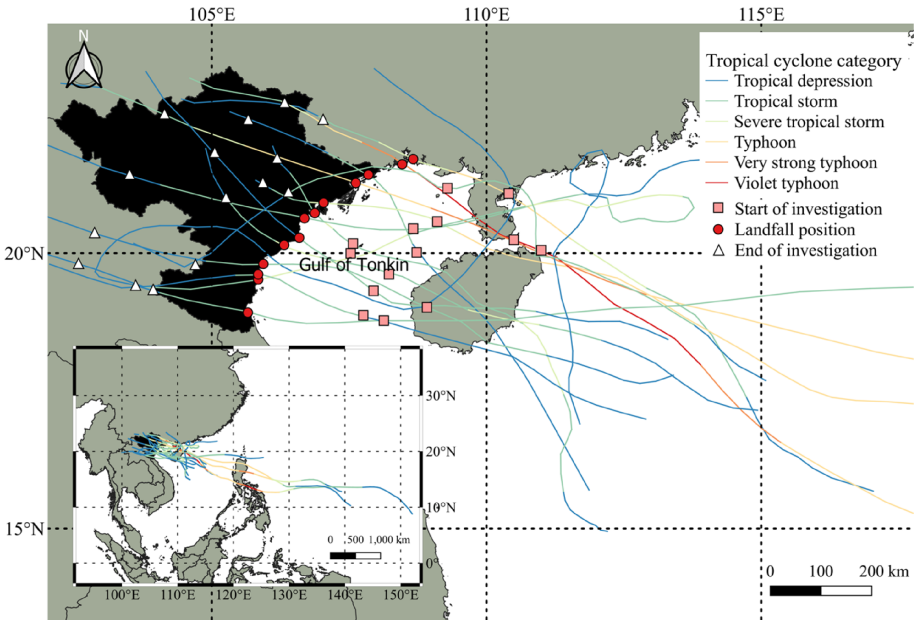

FIGURE 1 Northern Vietnam (black) with the 14 tropical cyclones (TCs) selected in this study. Red dots denote landfall locations, and pink squares and white triangles denote the locations of selected TCs at the start and end of this investigation, respectively.

2017. The IPET showed the best performance; however, it requires input of radius of maximum winds (R_{max}), which is not readily available for all historical tracks in the WNP basin. The R-CLIPER model requires the least storm track input (storm position and maximum wind speed) and had comparable performance to P-CLIPER and PHRaM. PHRaM utilizes R-CLIPER as a base and adds a topography component for asymmetry but demonstrated marginal improvement over R-CLIPER and with significant computational expense. Furthermore, these parametric TC rainfall models are fitted using TCs mostly in the United States, their performance in other regions need to be evaluated and calibrated using local historical data.

Our study aims to arrive at an improved parametric TC-induced rainfall model for the specific application in Northern Vietnam coast. Given the computation simplicity of R-CLIPER requiring only track information and its comparable performance, it was used as our starting TC-induced rainfall model. We first fit the existing R-CLIPER using historical TC events landfalling in the Northern Vietnam region to develop a locally calibrated R-CLIPER. We further introduce a quadrant-level redistribution into the calibrated R-CLIPER version to account for rainfall asymmetry. Asymmetry in TC rainfall is known to be affected by factors such as vertical wind shear (VWS), TC motion, and topography. Wingo and Cecil (2010) observed that in the Northern Hemisphere, TC-induced rainfall is more concentrated in the downshear left region, particularly under stronger shear conditions. However, Yu et al. (2015, 2017) may shift to the upshear region upon landfall under weaker shear conditions. Chen, Wang, and Yen (2006) earlier found that rainfall maxima in the WNP basin are often seen in the forward quadrant of TC motion. This suggests that the direction of TC motion and VWS magnitude can be used to assess asymmetry. TCs after landfall also typically experience a significant reduction in overall rainfall due to the loss of moisture supply; however, this can be complicated by topography and ascent slope of the mountains (Smith & Barstad, 2004). As such, the dominant rainfall quadrant may differ before and after landfall (Chan et al., 2019; Yu et al., 2015, 2017). For instance, in one of the three TC groups analyzed by Chan et al. (2019), the dominant rainfall quadrant shifted from the downward left (DL) quadrant before landfall to the forward left (FL) quadrant after landfall.

Therefore, this study focuses on producing a calibrated R-CLIPER suitable for TC-induced rainfall in the Northern Vietnam region, incorporating quadrant-level asymmetry accounting for the influence of VWS and landfall with respect to the TC forward motion. Sections 2 and 3 detail the input datasets and methodology for developing the asymmetric TC rainfall model, which is then followed by the evaluation of performance at domain, quadrant, and grid-level scales in Section 4. Section 5 presents the main conclusion of this study.

2 | DATA

2.1 | TC track data

The International Best Track Archive for Climate Stewardship (IBTrACS) project (Knapp et al., 2010; Knapp et al., 2018) is used as the source data for TC track information in this study. The IBTrACS best tracks provide 3-hr temporal information on such as latitudes, longitudes of the TC center, central pressure, and 1-minute maximum wind speed (V_m). 39 TCs made a landfall onto the Northern Vietnam region over 2001 to 2021 from which a total of 14 TCs are selected (see Table 1 and Figure 1). The selection is based on TCs meeting the criteria that they maintained themselves for at least 12 hr for both before and after landfall, that is, of sufficient duration and therefore impact. Thus, we investigated a consistent 24-hr span centered with respect to landfall for extraction of observed rainfall profiles. The TCs are categorized into six groups following RSMC Tokyo's Tropical Cyclone Intensity Scale (Chen, Wang, & Yen, 2006).

The majority of the 14 selected TCs are tropical storms. TY Rammasun, the strongest TC in the study, was identified as a violent typhoon while approaching Northern Vietnam but weakened to a severe tropical storm at landfall. Although these TCs made prior landfalls in the Philippines or/and China, they could re-intensify while travelling across the Gulf of Tolkin before landfalling onto Northern Vietnam coast. The track data are interpolated via natural cubic spline into 30-min time intervals for consistency with the observed rainfall data described next.

2.2 | Observed rainfall data

Rainfall intensity associated with the passage of the selected 14 TCs is obtained from the Global Precipitation Mission (GPM), a NASA project that uses satellites to measure precipitation globally (Huffman et al., 2014). The GPM data used here are the Integrated Multi-satellite Retrievals for GPM Final Run product, which combines satellite microwave precipitation estimates with other rainfall data from rain gauges at available locations. The GPM data have a spatial resolution of $0.1^\circ \times 0.1^\circ$ (approximately 11 km for Northern Vietnam region) and the 30-min temporal resolution is selected for our study. We investigate rainfall associated with the landfalling TCs considers over a 24-hr period comprising

TABLE 1 Summary of selected tropical cyclones (TCs) in the study. The category refers to the RSMC's Intensity Scale with maximum V_m over the 24-hr period shown. The cumulative rainfall over 24-hr period is computed covering up to 500 km.

Name	Year	Category (at landfall)	Maximum category during 12 hr prior to landfall	Maximum V_m (knots)	Cumulative rainfall (km^3)
Durian	2001	Severe tropical storm (STS)	Typhoon (TY)	75.3	33.5
Toraji	2007	Tropical depression (TD)	TS	35.2	14.4
Nesat	2011	Tropical storm (TS)	STS	60.4	41.4
Kujira	2014	TS	TS	48.0	14.4
Rammasun	2014	STS	Violent typhoon	119	40.3
Kalmaegi	2014	TY	TY	80.0	64.6
Mirinae	2016	STS	TY	65.0	24.7
Dianmu	2016	TS	TS	44.3	35.1
Son-Tinh	2018	TS	STS	50.0	25.0
Bebinca	2018	TS	STS	54.2	22.4
Mun	2019	TS	TS	35.2	24.1
Wipha	2019	TS	STS	55.6	22.9
Sinlaku	2020	TS	TS	35.2	28.8
Koguma	2021	TD	TS	35.0	27.6

12 hr before and 12 hr after landfall. The starting locations at 12 hr before landfall are also generally within 500 km of landfall (see Figure 1).

For the recalibration of the R-CLIPER model, mean radial rain profiles in 10-km annular bins as processed from the observed GPM-gridded data, covering up to 500 km from the TC center are used. This provides the data for an axisymmetric representation of the TC-induced rainfall. For consideration of quadrant asymmetry, the observed GPM-gridded rainfall is accumulated by quadrants to determine quadrant rainfall weights with respect to the TC motion.

2.3 | Vertical wind shear data

The VWS is used to categorize the shear influence on the rainfall asymmetry. The wind profiles associated with the selected TCs at two pressure levels, 850 and 200 hPa, are obtained from the fifth-generation reanalysis (ERA5) for global climate and weather from the European Center for Medium-Range Weather Forecasts (Hersbach et al., 2023). The ERA5 reanalysis provides hourly wind profiles at a spatial resolution of 0.25° × 0.25°. The zonal and meridional winds at both levels are temporally linearly interpolated to 30-min time interval, before averaging over an area of 500 km radially from the TC center at each timestep. The VWS is then calculated as the magnitude of the vector differences of these area-averaged vector winds at 850- and 200-hPa levels, following Corbosiero and Molinari (2002).

3 | METHODOLOGY

3.1 | R-CLIPER model

The R-CLIPER model was originally developed using rainfall data from 482 TCs that occurred globally from 1988 to 2002 (Lonfat et al., 2004; Marks & DeMaria, 2003). Axisymmetric radial profile for the rain rates (TRR) takes the form

$$TRR(r,V_m)=\begin{cases} T_0+(T_m-T_0)\dfrac{r}{r_m}, r<r_m \\ T_m\exp\left(-\dfrac{r-r_m}{r_e}\right), r\geq r_m \end{cases} \quad (1)$$

where $TRR(r,V_m)$ is the rainfall intensity (mm/hr) at the radial distance r from the TC center. The radial intensity profiles are characterized by four parameters: T_0 and T_m (both in mm/hr) as representing the rainfall intensity at the center and the maximum rainfall intensity at distance r_m (in km), respectively, while r_e characterizes the exponential tail behavior of the rainfall. The R-CLIPER further assumes linear relationships for T_0, T_m, r_m, and r_e with a normalized maximum wind U, where U takes the following form:

$$U=1+\frac{V_m-35}{33} \quad (2)$$

here, V_m is 1-min maximum wind speed in knots as, for example, interpolated from the IBTrACS best tracks.

Default linear coefficients for the four parameters available from the National Hurricane Centre (NHC) are as follows (coefficients for T_0 and T_m are updated to units of mm/hr): $T_0 = -1.16 + 4.19U$, $T_m = -1.69 + 5.08U$, $r_m = 64.5 - 13.0U$, $r_e = 150 - 16.0$. This version of R-CLIPER is referred hereafter as the NHC.

3.2 | Parametric TC-induced rainfall model for northern Vietnam

3.2.1 | Recalibration of the R-CLIPER model

The four parameters (T_0, T_m, r_m, and r_e) from each of the 14 historical TCs were extracted from the axisymmetric rain rate radial profiles processed using the GPM data described above. As we have radial profiles processed at each of 48 timestamps (30-min time intervals in total over 24 hr) for each of TC events, we then have a total of 672 profiles for the recalibration of the four parameters. Figure 2 presents the observed data between each pair of the four parameters and U, with the data plotted via boxplots over U bins to reduce the scatter. We generally see a larger scatter for $U < 2$, as most of the historical TCs fall into this range of wind intensity. Two different U bin sizes, 0.1 for $U < 2$ and 0.25 for $U \geq 2$ are then used in Figure 2. We note the data distributions in several U bins are skewed. The medians of each parameter (thick horizontal lines within the boxplots) in each binned U are therefore used in fitting with. The blue lines in Figure 2 represent the best-fit relationship for each rainfall parameter, detailed as follows: $T_0 = 3.11 + 4.98ln(U)$,

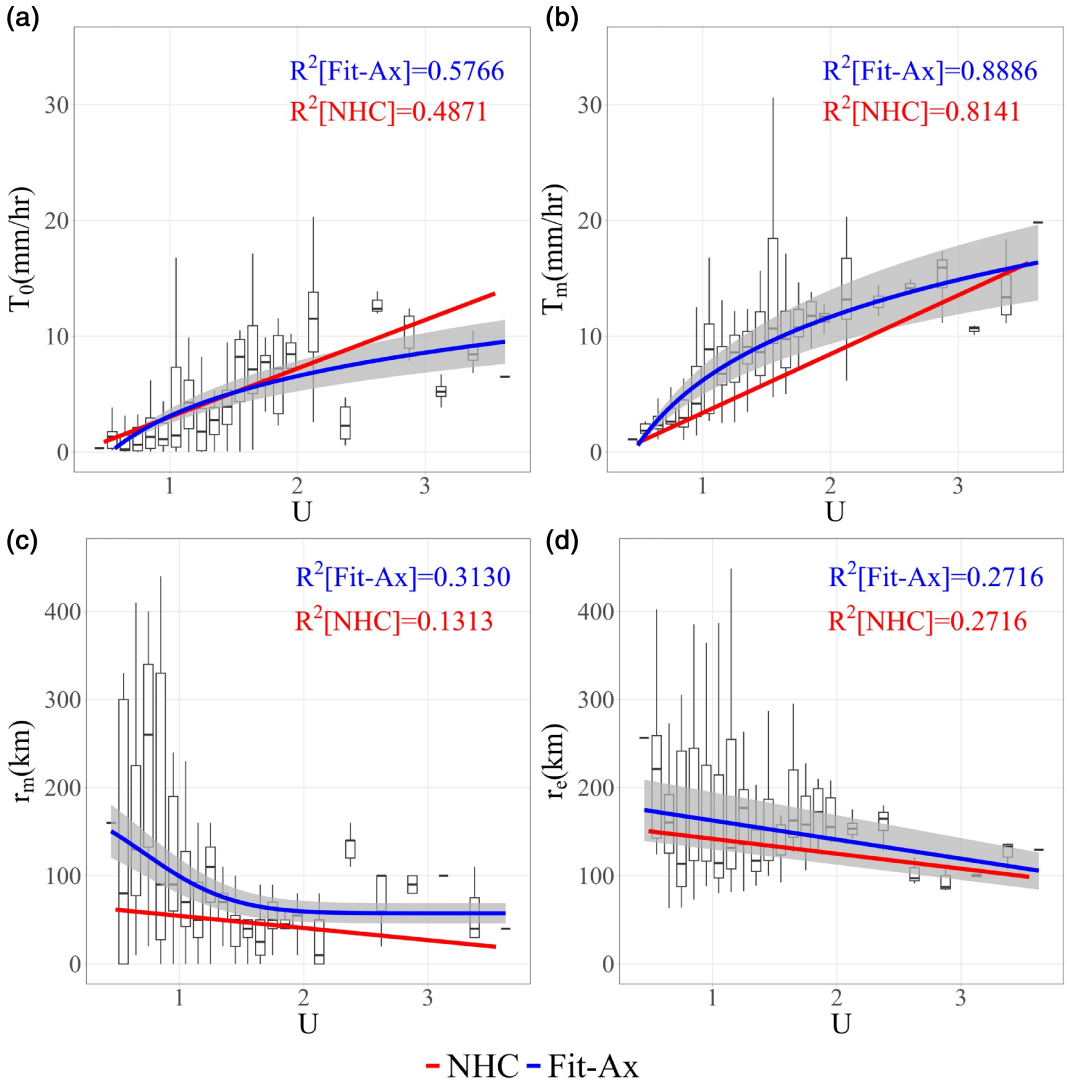

FIGURE 2 Boxplots showing GPM derived rainfall profile parameters against U bins. Red lines indicate NHC. Blue lines indicate Fit-Ax with shaded grey areas indicating ±20% prediction bands. R^2 values for both versions are shown. Box boundaries correspond to 25th and 75th quantiles, with the solid interior lines and whiskers depicting the medians and data ranges, respectively.

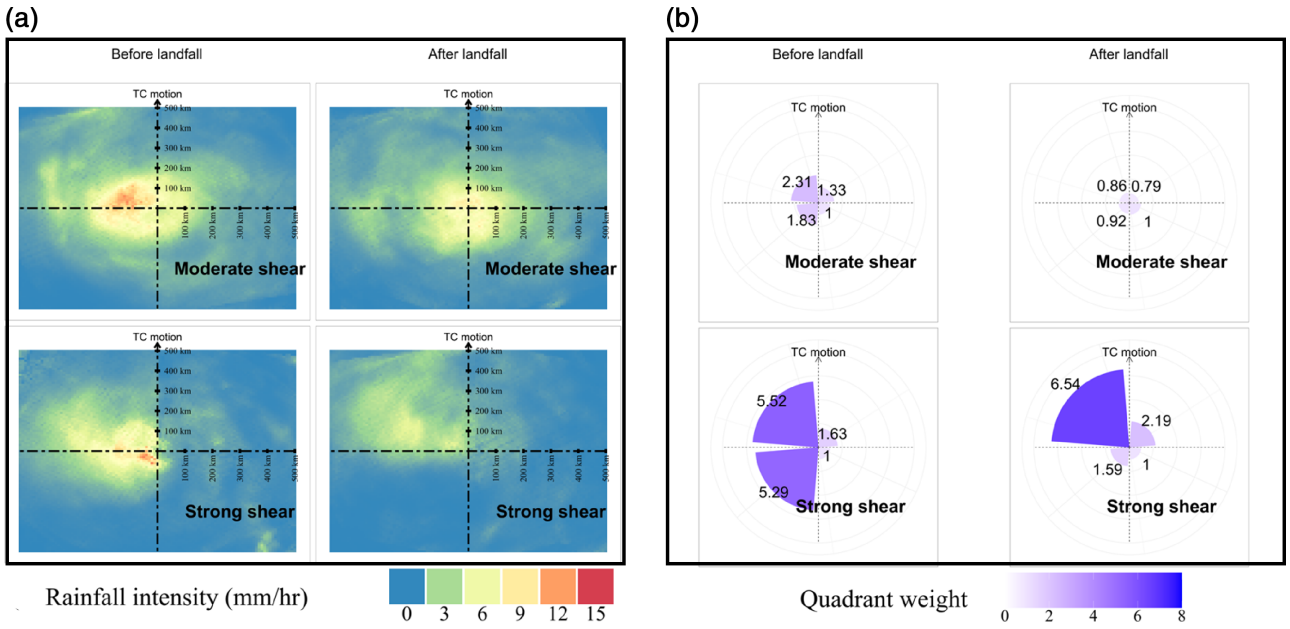

FIGURE 3 (a) Grid-level average rainfall intensity and (b) quadrant weights (w_Q) for rainfall volume under moderately shear (upper panels) and strong shear (lower panels) environments during the before- and after-landfall periods, with the TC motion as a reference direction (upward).

$T_m = 6.20 + 7.90ln(U)$, $r_m = 57.4 + 114exp(-U^2)$, and $r_e = 184 - 21.7U$. We refer to this recalibrated R-CLIPER model as the Fitted version (Fit-Ax) hereafter.

Fit-Ax (plotted as blue lines) show improved R^2 values for T_0, T_m and r_m over the NHC (red lines). For example, R^2 of T_m has improved from 0.814 to 0.889, indicating the variation of the median being better captured. Fit-Ax also takes the logarithmic form for both T_0 and T_m, and exponential for r_m with U, while r_e remains linear with U. The ±20% prediction bands for Fit-Ax (shaded gray areas in Figure 2) cover a large faction of 25^{th}–75^{th} quantiles, especially for T_m, and to a lesser extent for T_0, r_m, and r_e.

3.2.2 | Developing quadrant asymmetry

To account for quadrant asymmetry, we further redistribute the quadrant rainfall intensity profiles from Fit-Ax using the quadrant weights (w_Q) calculated from the GPM data (Figure 3). The TC forward motion is used as a reference to define quadrants as forward right (FR), FL, downward right (DR) and DL.

Previous studies by Corbosiero and Molinari (2002), and Cecil (2007) categorized the VWS into low (0–5 m/s), moderate (5–10 m/s), and strong (>10 m/s) environments. We chose two categories following Paterson et al. (2005) as moderate (VWS ≤10 m/s) and strong (VWS >10 m/s) with 58% of our data in the moderate category. In both categories, it is found that the DR quadrant tends to experience the least amount of rainfall volume before landfall. We therefore assign a unit weight (magnitude of 1) and with other w_Q referenced from it. The average grid-level rainfall intensity from the selected 14 TCs is shown in Figure 3a for different VWS groups and landfall periods. It is then used to calculate observed rainfall volumes for each quadrant to obtain w_Q in Figure 3b. The asymmetry is generally more prominent in a strongly sheared environment than moderately sheared environment as agreed with Wingo and Cecil (2010). The quadrant weights reveal that more pronounced rainfall volume is present in the left quadrants (FL and DL) before landfall in both VWS categories. This agrees with the study of Chan et al. (2004) showing that the convection in TCs landfalling onto South China was stronger on the left of TC center before landfall resulting in more amount of rainfall there. As seen from Figure 3, this holds for both VWS categories but to a significantly lesser extent for the moderately sheared environment.

We therefore calculate quadrant-asymmetric TC rainfall intensity as

$$TRR_Q(r, V_m) = \frac{w_Q}{w_{FL} + w_{FR} + w_{DL} + w_{DR}} \times 4\, TRR_{Ax}(r, V_m) \quad (3)$$

where $TRR_Q(r, V_m)$ is the quadrant-level rainfall intensity at distance r from the TC center and $TRR_{Ax}(r, V_m)$ is Fit-Ax described in Section 3.2.1. Subscript Q denotes the quadrant, that is, FL, FR, DL, or DR with corresponding to w_Q from Figure 3b. This version is termed Fitted version with asymmetry (Fit-As) hereafter.

3.3 | Performance metrics

The performances of the three versions (NHC, Fit-Ax and Fit-As) are evaluated using statistical metrics of model skill at both domain, quadrant, and grid scales (see Appendix A for metric definitions). The domain-level analysis evaluates the total rainfall, defined as the accumulated rainfall over a 12-hr period before and after landfall, for (i) the 500-km entire TC domain, (ii) the inner core (0–200 km), and (iii) the outer region (200–500 km) as following Yu et al. (2022). Metrics used are the root-mean-square error (RMSE) and Bias. The quadrant-level evaluation considers total quadrant rainfall during the 12 hr before and after landfall, and the 24-hr average quadrant rainfall intensity in 20-km radial bins up to 500 km. Hence, the quadrant intensity evaluation has a total of 25 annular quadrant bins for each of 14 TC events, giving a total of 350 data points per quadrant in the calculation of each metric. Rainfall intensity rather than volume is used to avoid uncertainties in the rainfall data being amplified in the larger annular bins. We use four metrics, RMSE, normalized root-mean-square error (NRMSE), Bias, and Willmott skill score (Skill), to access the performance for the quadrant rainfall estimates. The grid-level evaluation focuses on pattern matching performance via using the threat scores (TS), equitable threat scores (ETSs), and Pearson coefficient correlations (PCC). The 24-hr total rainfall depth at the default $0.1^\circ \times 0.1^\circ$ GPM spatial resolution within the domain of the 500-km radial distance from the TC center is used. Hence, we have a total of over 6,300 data points for each TC in the grid-level pattern matching.

4 | EVALUATION OF THE PARAMETRIC TC RAINFALL MODEL

4.1 | Domain-level performance analysis

Figure 4 compares the estimated 12-hr total rainfall depths before and after landfall against the observed GPM data. As Fit-As only redistributes the rainfall calculated from Fit-Ax, their 12-hr total rainfalls are identical, and referred to as Fit-Ax/Fit-As. Over the entire 500-km domain, Fit-Ax/Fit-As improves the prediction from NHC on both RMSE and Bias measures for both before and after-landfall periods (Figure 4a–d). The Bias improvement is significant with the before- and after-landfall magnitudes reduced by 67.3% and 43.4%, respectively.

In the inner core, which accounts for the majority of the total rainfall, Fit-Ax/Fit-As shows also much improved agreement with observed data compared with NHC before landfall, especially for the larger rainfall TCs with >400 mm inner core total rainfall (Figure 4e,f). RMSE and Bias magnitude reduce from 107.46 to 93.88 mm and from 77.97 and 58.6 mm, respectively. For the after-landfall period (Figure 4g,h), the Fit-Ax/Fit-As results show a slightly greater scatter than the NHC results. This larger scatter is generally caused by overestimation for TCs with an inner core rainfall of <200 mm, while NHC generally performs better for these TCs. Conversely, Fit-Ax/Fit-As provides better agreement for TCs with >200-mm inner core total rainfall after landfall. For the outer region, Fit-Ax/Fit-As outperforms NHC (Figure 4i–l), with significant improvement clearly seen in both RMSEs and Biases for both before- and after-landfall periods. This comparison demonstrates that Fit-Ax/Fit-As consistently reduces prediction error and bias as compared with NHC for both before- and after-landfall periods. The only exception is for TCs with <200 mm the inner core total rainfall after landfall, where Fit-Ax/Fit-As tends to overestimate.

4.2 | Quadrant-level performance analysis

4.2.1 | Quadrant-level total rainfall

We further evaluate the effective of the quadrant-level weights introduced in Section 3.2.2 for incorporating asymmetry into Fit-As. Figures 5 and 6 compare the 12-hr total rainfall estimated from the axisymmetric NHC and Fit-Ax, and the asymmetric Fit-As for before and after landfall, respectively. These figures also include four statistical metrices of RMSE, NRMSE, Bias, and Skill for each version in different quadrants. Overall, NHC is likely to underpredict total rainfall beyond the lower 25% of the rainfall range (Figures 5 and 6, left panels) and with especially large Biases on the FL and DL quadrants. Fit-Ax performs better overall but tends to overpredict for TCs with lower total rainfalls of ~20 mm. This generally resembles the findings in Figure 4a–d. Since Fit-As redistributes the domain-level predictions from Fit-Ax based on quadrant asymmetry seen in the observed rainfall data, it does not correct the domain-level prediction errors from Fit-Ax. In particular, the quadrant-specific weights will scale up the Fit-Ax rainfall in the FL and DL quadrants before landfall, and especially for TCs in a strong shear environment, after landfall. Consequently, the overestimation of Fit-Ax for TCs in lower rainfall ranges may be exacerbated in those quadrants. This underscores a limitation of the quadrant-level weights, as they are not designed to correct for prediction errors of the domain-level total rainfall by Fit-Ax.

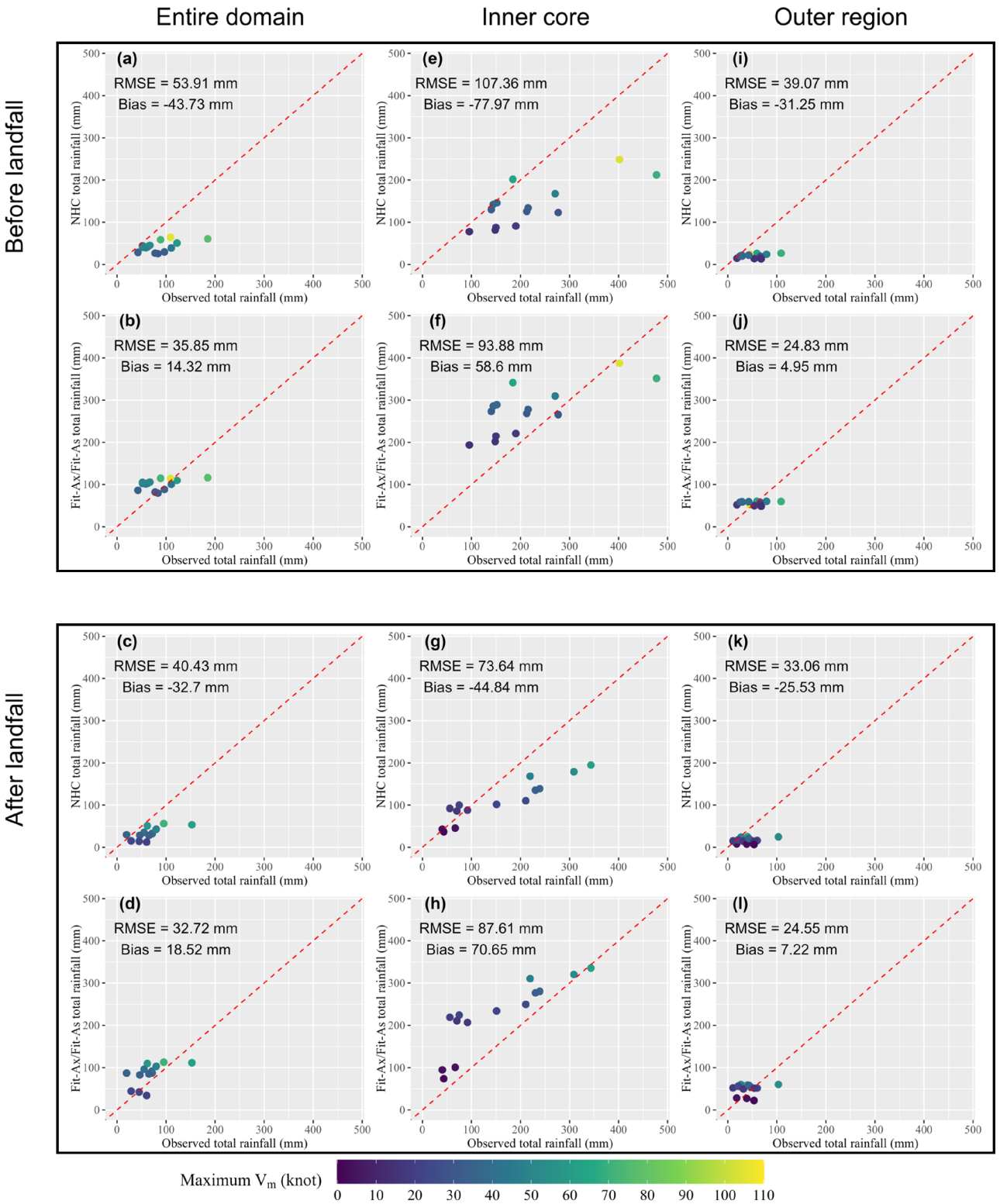

FIGURE 4 Comparison of predicted 12-hr total rainfall against observed rainfall for NHC and Fit-Ax/Fit-As. (a–d) The entire domain (500-km radial distance from TC center). (e–h) The inner core (within 200-km radial distance from TC center), and (i–l) The outer region (200–500-km radial distance from TC center). The colored scale is the max V_m in knots during the 12-hr period (either before or after landfall).

Despite this limitation, a notable improvement is seen in representing asymmetry across the four quadrants both before and after landfall. For the before-landfall total rainfall, Fit-As shows a systematic increase in the estimates compared with Fit-Ax in the dominant FL and DL quadrants. This reduces the overall RMSE, NRMSE, and Bias in the FL quadrant, compared NHC and Fit-Ax (Figure 5a). Fit-As also improves Skill from Fit-Ax in the

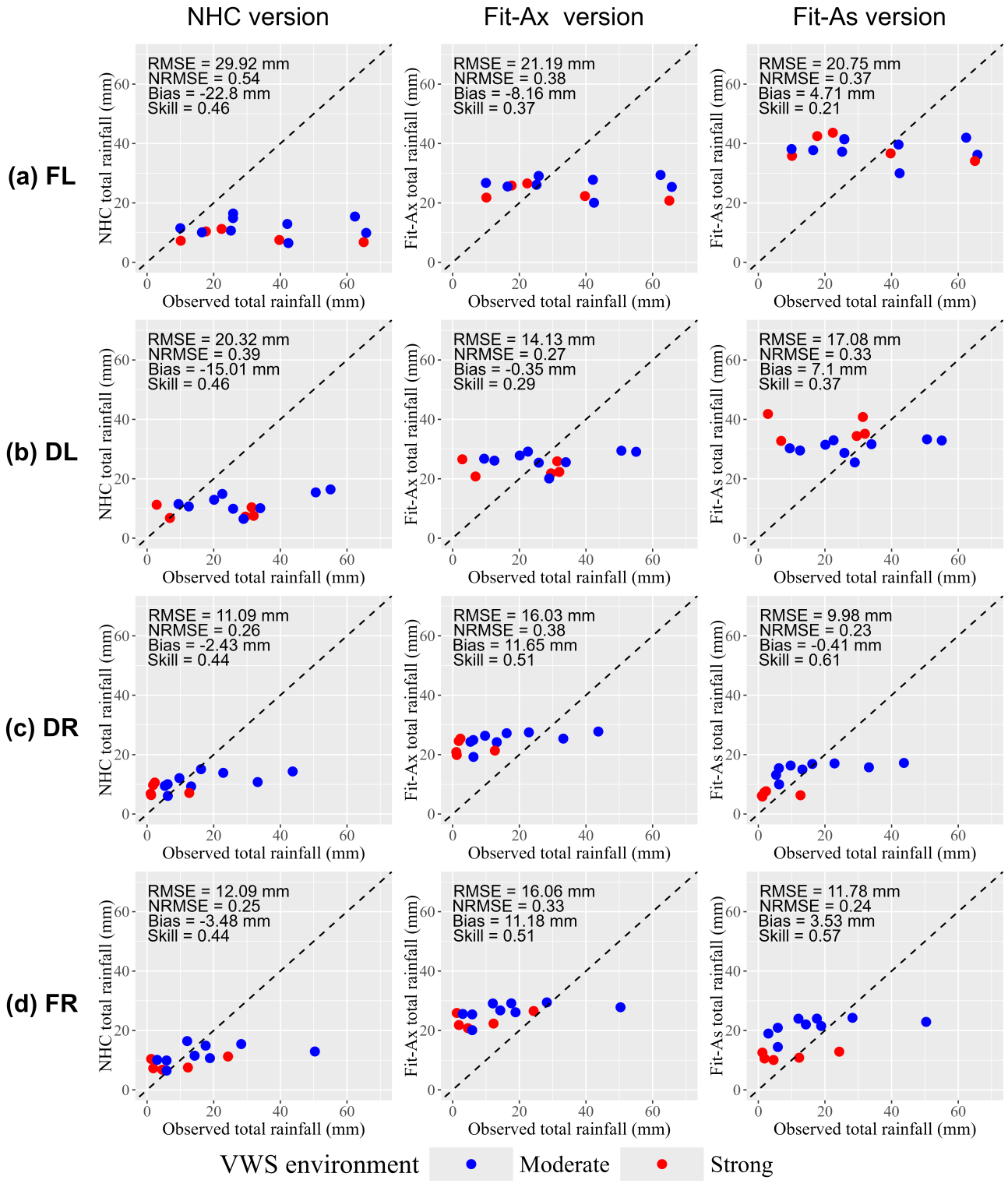

FIGURE 5 Comparison of the predicted quadrant-level 12-hr total rainfall against the observed rainfall before-landfall period for NHC, Fit-Ax and Fit-As. (a–d) indicate the forward left (FL), downward left (DL), downward right (DR), and forward right (FR) quadrants.

DL quadrant (Figure 5b), reducing the prediction error across the observed data range. Correspondingly, Fit-As scales down the total rainfall estimates from Fit-Ax in the DR and FR quadrants (Figure 5c,d), reducing errors (11.8%–39.5%), and bias magnitude (68.5%–96.5%) in the prediction. The model performance across the entire observed rainfall ranges is improved as seen in the increased Skill value from both NHC and Fit-Ax. In the after-landfall period, only TCs in the strong shear environment (indicated as red dots in Figure 6)

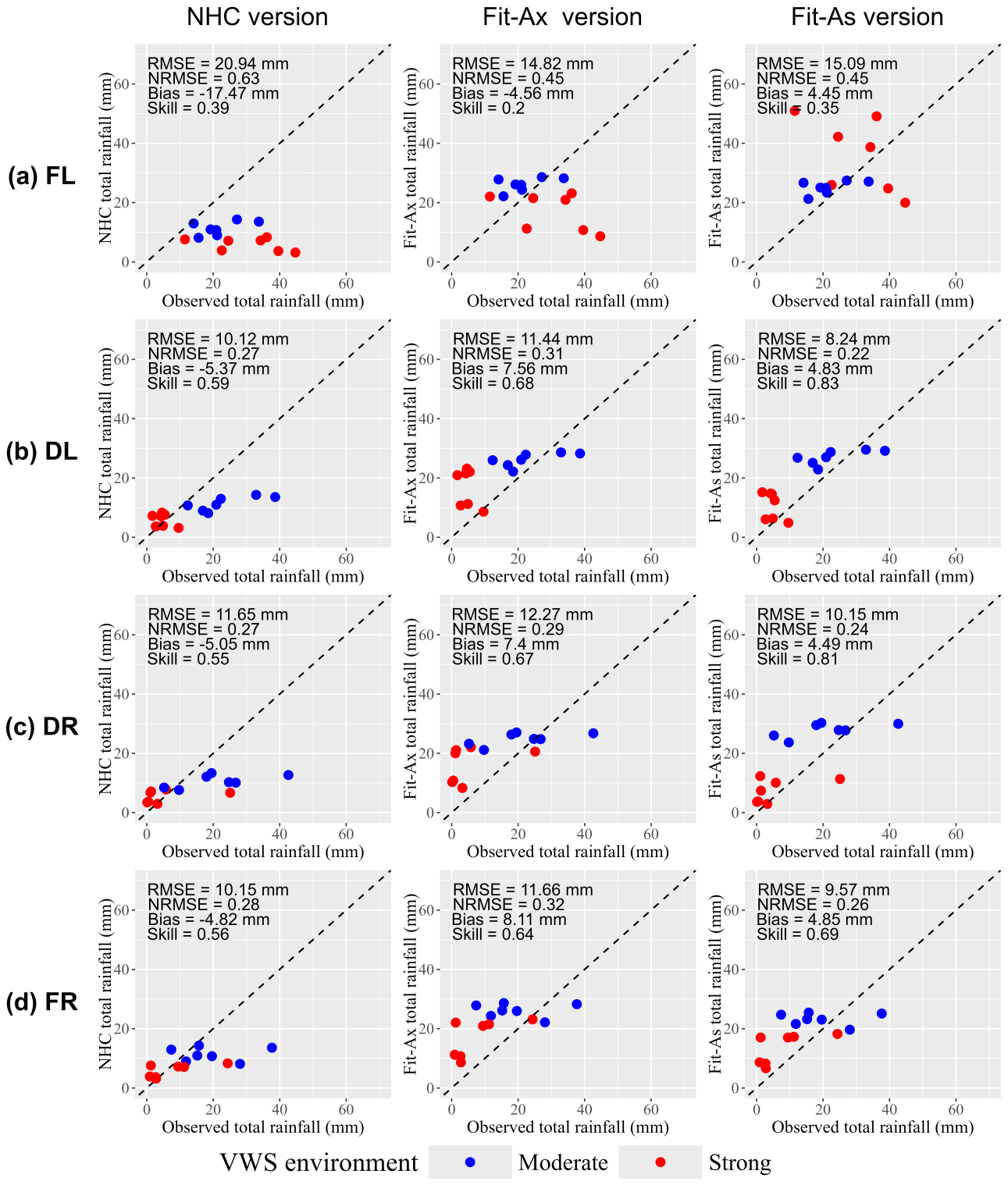

FIGURE 6 Comparison of the predicted quadrant-level 12-hr total rainfall against the observed rainfall after-landfall period for NHC, Fit-Ax and Fit-As. (a–d) indicate the forward left (FL), downward left (DL), downward right (DR), and forward right (FR) quadrants.

experienced clear rainfall redistribution across the quadrants. This redistribution is reflected in increased total rainfall in the FL quadrant (Figure 6a) and reductions in the other quadrants (Figure 6b–d). The Fit-As predictions for the FL quadrant enhanced overall prediction Skill (increased from the lowest at 0.20 to 0.35) and addressed the underprediction seen with Fit-Ax for TCs in the strong shear conditions. However, Fit-As shows a slightly larger RMSE compared with Fit-Ax. This is likely due to significant overprediction for the single TC with ~10 mm

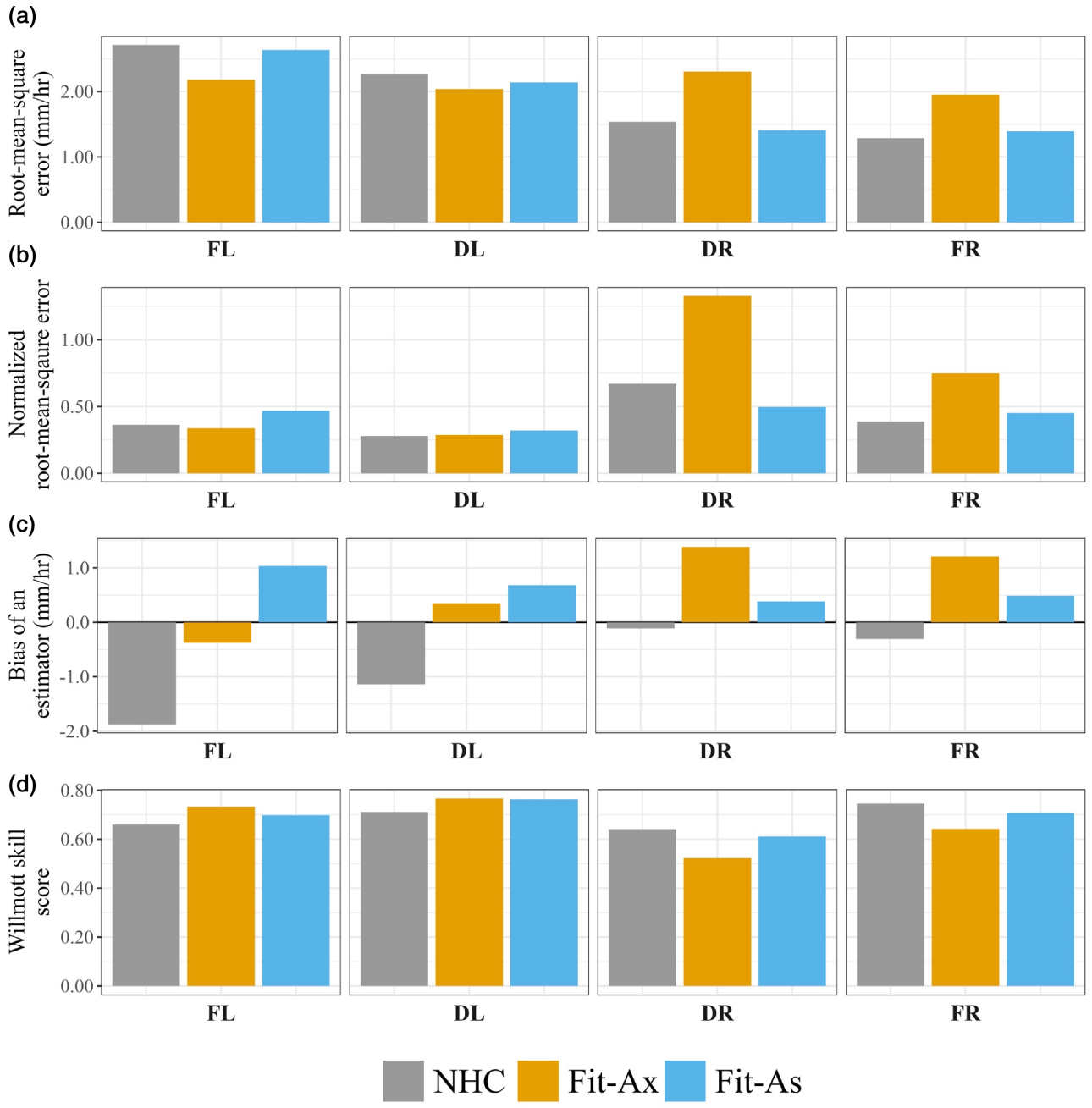

FIGURE 7 Comparison of quadrant-level metrics for 24-hr average rainfall intensity of (a) Root-mean-square error (RMSE), (b) Normalized root-mean-square error (NRMSE), (c) Bias of an estimator, and (d) Willmott skill score.

of the observed total rainfall for this FL quadrant (Figure 6a). Conversely, reductions in the DL, DR, and FR quadrants for TCs in a strong shear environment result in substantial improvements across the prediction errors, Bias and Skill, providing better performance compared with Fit-Ax.

Overall, we have four quadrants and four metrics, that is, 16 combinations for each rainfall estimates for both before and after landfall quadrant rainfall. Fit-As performs best in 11 for before landfall and 14 for after landfall. NHC and Fit-Ax have 3 and 4 combinations being best.

4.2.2 | Quadrant-level average rainfall intensity

Figure 7 presents the quadrant-level evaluation of average rainfall intensity from NHC, Fit-Ax, and Fit-As over the 14 TC events via the four metrics of RMSE, NRMSE, Bias, and Skill. The performance at quadrant-level varies with the quadrant considered. In the left quadrants with larger rainfall, that is, FL and DL quadrants, Fit-Ax tends to have the best performance across the four measures, with more pronounced improvement from NHC in all

Version	RMSE (mm/hr)	NRMSE	Bias (mm/hr)	Skill
NHC	2.090	0.420	−1.019	0.682
Fit-Ax	2.139	0.629	0.480	0.676
Fit-As	2.018	0.437	0.708	0.694

TABLE 2 Quadrant weighted performance for the 24-hr average rainfall intensity.

four metrics. There is a 3.0%–19.6% improvement in RMSE, NRMSE, and Skill in both left quadrants. We see the largest improvement in Bias of 69.3% and 80.2% for the DL and FL quadrants, respectively. Fit-As shows similar improvements in RMSE and Skill (2.9%–7.4%) over the left quadrants. In the right quadrants with less rainfall (DR and FR quadrants), NHC outperforms the other two across all four measures, with Fit-Ax being the worst. For example, in the FR quadrant, while the Bias magnitudes of NHC and Fit-As are relatively similar at 0.304 and 0.413 mm/hr., the magnitude of Fit-Ax is much larger at 1.21 mm/hr. The same trend in Bias magnitudes hold for the DR quadrant. The above observations, that is, Fit-Ax being generally the best and worse is the left and right quadrants, respectively, are likely due to its calibrated axisymmetric fitting coefficients being more driven by higher rainfall in the left quadrants. Fit-As corrects this overestimation via the quadrant redistribution weights, correcting the large bias introduced by the Fit-Ax in the right quadrants.

A more representative comparisons at the quadrant-level metrics are obtained by weightage with observed 24-hr quadrant rainfall volume, as shown in Table 2. Both Fit-Ax and Fit-As show significant improvement in Bias over NHC. For both RMSE and Skill, the performances of NHC and Fit-As are comparable with Fit-As being slightly better. In terms of NRME, the Fit-As value has been significantly improved from the Fit-Ax value.

4.3 | Grid-level performance analysis

The grid-level performance of the three versions was evaluated using the TS, ETS, and PCC. Both TS and ETS are used for assessing pattern matching trends with higher scores indicating better pattern matching performance. The ETS further removes contribution from hits by chance in random forecasts (Gandin and Murphy, 1992) and allows a better representation of performance at lower rainfall thresholds. Therefore, the ETS has been used to evaluate patterns of TC-induced rainfall predictions as reported in various studies (e.g., Brackins & Kalyanapu, 2020; Osuri et al., 2020; Sun & Liang, 2020). In our evaluation below, the total 24-hr rainfall depths induced by the 14 TCs are categorized into three groups: Heavy (25–50 mm), Storm (50–100 mm), and Large Storm (100–250 mm), based on the study of Li et al. (2015). Thus, rainfall thresholds ranging from 0 to 250 mm of the rainfall depths are used in our TS and ETS analysis with the GPM spatial resolution of $0.1^\circ \times 0.1^\circ$.

Figure 8a The TS values of Fit-As are greater than those of the other two versions over 10 to 250 mm of the rainfall thresholds. At 100-mm rainfall threshold (upper bound of Storm group), the Fit-As has a TS of 0.343, followed by those of Fit-Ax and NHC at 0.270 and 0.123, respectively. Thus, the performances of both Fit-Ax and Fit-As are significantly better in pattern matching than that of NHC with Fit-As being the best. The TS values expectedly reduce with increasing rainfall threshold. At the larger 250-mm rainfall threshold area (upper bound of Large Storm), the TS values of Fit-As and Fit-Ax are 0.078 and 0.023, respectively, with both still significantly higher than the TS of 0.004 from NHC.

The ETS values shown in Figure 8b indicates that Fit-As performs better than NHC beyond the rainfall threshold of 20 mm, while outperforming Fit-Ax over the full range of rainfall thresholds shown. Their maximum ETS of 0.236 and 0.299 for Fit-Ax and Fit-As are both at the 90-mm threshold, respectively, that is, higher than the maximum ETS of 0.2 reported by Brackins and Kalyanapu (2020) in their evaluation of the reviewed four parametric TC rainfall models (R-CLIPER, P-CLIPER, IPET, and PHRaM) for the Atlantic basin. The ETS trends of Fit-Ax and Fit-As are similar, and both decreasing around the same rate after their peaks until the threshold of 250 mm.

Figure 9 presents PCC analysis of grid-level rainfall depths between the predicted and observed via the event-level PCCs and averaged PCC over all 14 events. Figure 9a shows that Fit-As provides the best prediction of the grid-level rainfall depths for 11 of the 14 TCs, with the highest PCC at 0.877 for predicted rainfall of TY Kalmaegi. The remaining three TCs have NHC performing the best for two of the three events and Fit-Ax the best for one event. For the 11 TC events where Fit-As performs the best, the largest improvement is seen in the tropical storm Mun, where the PCC is 0.549 compared with NHC of 0.195. When averaged over the 14 TC events, Figure 9b indicates that Fit-As outperforms with a mean PCC of 0.653. This is followed by Fit-Ax and the NHC at 0.553 and 0.548, respectively.

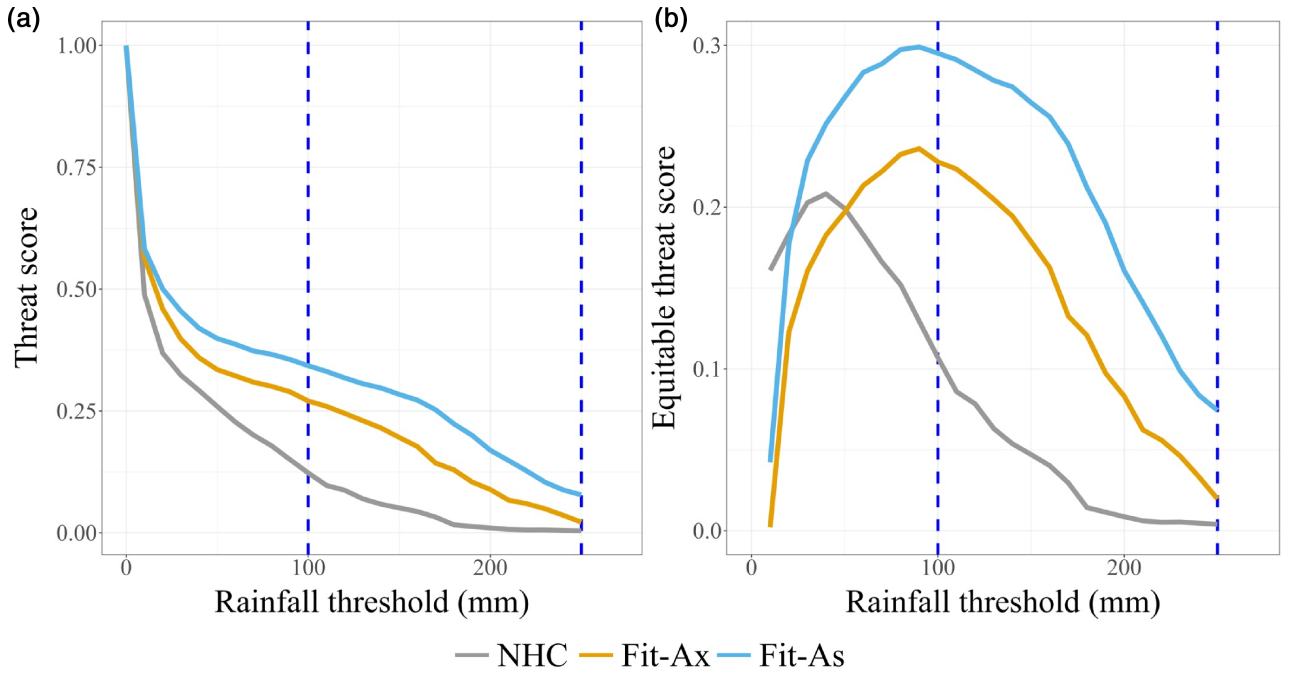

FIGURE 8 Threat score and equitable threat score (ETS) for rainfall thresholds from 0 to 250 mm. Vertical dashed lines represent the thresholds at 100 and 250 mm.

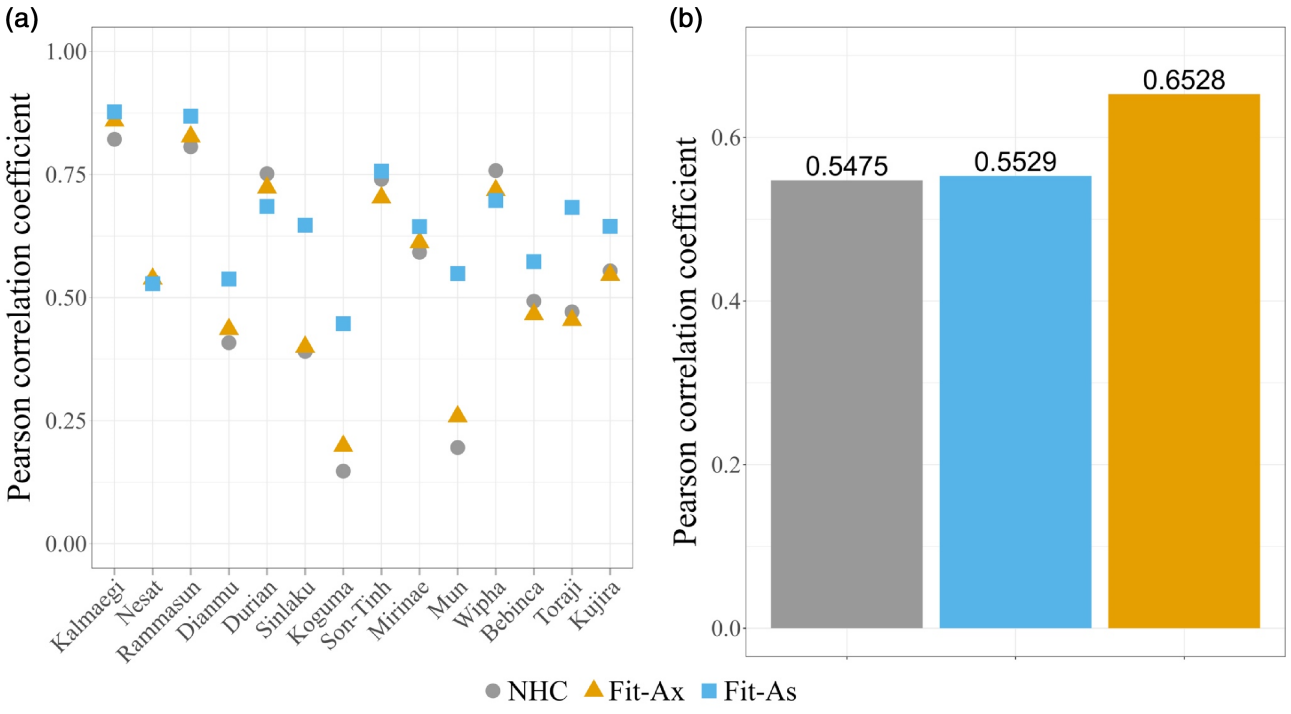

FIGURE 9 Comparison of Pearson correlation coefficients for NHC, Fit-Ax, and Fit-As of 24-hr rainfall depth. (a) event-level performance (order of TCs is from the maximum total rainfall to the minimum) and (b) averages of 14 events.

5 | CONCLUSION

This study improves on the existing R-CLIPER parametric TC-induced rainfall model for a specific application in Northern Vietnam coast. Totally 14 historical TC events landfalling in the Northern Vietnam region are used to firstly recalibrate the base R-CLIPER model (NHC) for local relationships between rainfall parameters and TC

track speed using GPM observed rainfall over the events. This produced a locally fitted axisymmetric (Fit-Ax) version from which we further introduced a quadrant-level redistribution to account for quadrant rainfall asymmetry (Fit-As) as based on the VWS and landfall (before/after). The performance of the three versions, NHC, Fit-Ax, and Fit-As, is then compared with GPM observations via domain, quadrant, and grid-level metrics.

Over the entire 500-km domain, Fit-Ax/Fit-As improves upon the total rainfall estimation from NHC, with notable reductions in RMSE and Bias magnitude for both the before and after periods. Fit-Ax/Fit-As also outperforms NHC for stronger TCs with inner core rainfall >200 mm. At the quadrant level, Fit-As generally outperforms Fit-Ax and NHC in reproducing the observed rainfall distribution. The 24-hr quadrant rainfall weighted metrics indicate that Fit-As significantly improves upon Bias from NHC and better overall in RMSE and Skill. The grid-level pattern matching using 24-h total rainfall shows Fit-As has the highest TS in rainfall threshold ranging from 10 to 250 mm (Heavy to Large Storm category). Its ETS is also the highest, except in the 10–20-mm rainfall threshold range. Lastly, the Pearson correlation measure also indicates that Fit-As is best for 11 out of 14 TCs used.

The above results indicate that Fit-As incorporating quadrant asymmetry outperforms NHC and Fit-Ax in reproducing the TC-induced rainfall in the Northern Vietnam coast. However, it should be noted that the sample size is limited due to our selection of longer persisting TCs (i.e., sustained for 12 h after landfall). Incorporation of shorter-lived TCs may improve on the before-landfall rainfall distribution but have limited value for after-landfall impact studies. In addition, TC characteristics can be unique for each basin and coastal topography. Therefore, while the presented methodology using quadrant asymmetry in Fit-As development as starting from the base R-CLIPER model have general applicability, local refitting should be performed for applications to other coastal areas frequented by TCs.

AUTHOR CONTRIBUTIONS

Warinthorn Angkanasirikul: Methodology; investigation; visualization; writing – original draft; formal analysis; resources; writing – review and editing; data curation; validation; conceptualization; software. **Wei Jian:** Writing – review and editing; supervision; data curation; validation; resources; conceptualization; formal analysis; methodology. **Edmond Yat-Man Lo:** Writing – review and editing; supervision; funding acquisition; conceptualization; formal analysis.

ACKNOWLEDGEMENTS

This research work was supported by a doctoral scholarship from the Nanyang Technological University via its Institute of Catastrophe Risk Management.

CONFLICT OF INTEREST STATEMENT

The authors declare that there are no conflicts of interest in this study.

DATA AVAILABILITY STATEMENT

The data that support the findings of this study are available from the corresponding author upon reasonable request.

ORCID

Warinthorn Angkanasirikul https://orcid.org/0000-0001-8129-9101

REFERENCES

Brackins, J.T. & Kalyanapu, A.J. (2020) Evaluation of parametric precipitation models in reproducing tropical cyclone rainfall patterns. *Journal of Hydrology*, 580, 124255. Available from: https://doi.org/10.1016/j.jhydrol.2019.124255

Cecil, D.J. (2007) Satellite-derived rain rates in vertically sheared tropical cyclones. *Geophysical Research Letters*, 34(2), L02811. Available from: https://doi.org/10.1029/2006GL027942

Chan, J.C., Liu, K.S., Ching, S.E. & Lai, E.S. (2004) Asymmetric distribution of convection associated with tropical cyclones making landfall along the South China coast. *Monthly Weather Review*, 132(10), 2410–2420. Available from: https://doi.org/10.1175/1520-0493(2004)132<2410:ADOCAW>2.0.CO;2

Chan, K.T., Chan, J.C. & Wong, W.K. (2019) Rainfall asymmetries of landfalling tropical cyclones along the South China coast. *Meteorological Applications*, 26(2), 213–220. Available from: https://doi.org/10.1002/met.1754

Chen, T.C., Wang, S.Y. & Yen, M.C. (2006) Interannual variation of the tropical cyclone activity over the western North Pacific. *Journal of Climate*, 19(21), 5709–5720. Available from: https://doi.org/10.1175/JCLI3934.1

Corbosiero, K.L. & Molinari, J. (2002) The effects of vertical wind shear on the distribution of convection in tropical cyclones. *Monthly Weather Review*, 130(8), 2110–2123. Available from: https://doi.org/10.1175/1520-0493(2002)130%3C2110:TEOVWS%3E2.0.CO;2

Davies, R. (2014) Severe floods in Vietnam after typhoon Rammasun. *FloodList*. [Online]. Available at: https://floodlist.com/asia/severe-floods-vietnam-typhoon-rammasun [Accessed 20 June 2022]

ESCAP/WMO Typhoon Committee. (2014) ESCAP/WMO *typhoon committee member report*. ESCAP-UN conference center. Available at https://www.typhooncommittee.org/9IWS/DOCS/Members%20Report/VIetnam/Country%20Report%202014_Vietnam_final.pdf [Accessed: 20 March 2022]

Gandin, L.S., & Murphy, A.H. (1992). Equitable Skill Scores for Categorical Forecasts. *Monthly Weather Review*, 120(2), 361–370. Available from: https://doi.org/10.1175/1520-0493(1992)120<0361:essfcf>2.0.co;2

Geoghegan, K.M., Fitzpatrick, P., Kolar, R.L. & Dresback, K.M. (2018) Evaluation of a synthetic rainfall model, P-CLIPER, for use in coastal flood modelling. *Nature Hazards*, 92(2), 699–726. Available from: https://doi.org/10.1007/s11069-018-3220-4

Hersbach, H., Bell, B., Berrisford, P., Biavati, G., Horányi, A., Muñoz Sabater, J. et al. (2023) *ERA5 hourly data on single levels from 1940 to present*. Reading: Copernicus Climate Change Service (C3S) Climate Data Store (CDS). Available from: https://doi.org/10.24381/cds.adbb2d47

Huang, X., He, L., Zhao, H. & Huang, Y. (2017) Characteristics of tropical cyclones generated in South China Sea and their landfalls over China and Vietnam. *Natural Hazards*, 88(2), 1043–1057. Available from: https://doi.org/10.1007/s11069-017-2905-4

Huffman, G., Bolvin, D., Braithwaite, D., Hsu, K., Joyce, R. & Xie, P. (2014) *Integrated Multi-satellite retrievals for GPM (IMERG), version 4.4*. Washinton, D.C: NASA's Precipitation Processing Center. [Online] Available at: ftp://arthurhou.pps.eosdis.nasa.gov/gpmdata/

Hung, M.K., Tien, D.D., Quan, D.D., Duc, T.A., Dung, P.T.P., Hole, L.R. et al. (2023) Assessment of use of blended radar-numerical weather prediction product in short-range warning of intense rainstorms in localized systems (SWIRLS) for quantitative precipitation forecast of tropical cyclone landfall on Vietnam's coast. *Atmosphere*, 14(8), 1201. Available from: https://doi.org/10.3390/atmos14081201

Institute of Strategy and Policy on Natural Resources and Environment (ISPONRE). (2009) *Vietnam assessment report on climate change (VARCC)*. Hanoi, Vietnam: Van hoa – Thong tin Publishing House.

Interagency Performance Evaluation Task Force (IPET). (2006) Performance evaluation of the New Orleans and Southeast Louisiana hurricane protection system draft final report of the interagency performance evaluation task force volume VIII – engineering and operational risk and reliability analysis.

Knapp, K.R., Diamond, H.J., Kossin, J.P., Kruk, M.C. & Schreck, C.J. (2018) International best track archive for climate stewardship (IBTrACS) project, Version 4.

Knapp, K.R., Kruk, M.C., Levinson, D.H., Diamond, H.J. & Neumann, C.J. (2010) The international best track archive for climate stewardship (IBTrACS) unifying tropical cyclone data. *Bulletin of the American Meteorological Society*, 91(3), 363–376. Available from: https://doi.org/10.1175/2009BAMS2755.1

Li, Q., Zhu, Q., Zheng, J., Liao, K. & Yang, G. (2015) Soil moisture response to rainfall in forestland and vegetable plot in Taihu Lake Basin, China. *Chinese Geographical Science*, 25, 426–437. Available from: https://doi.org/10.1007/s11769-014-0715-0

Lonfat, M., Marks, F.D. & Chen, S.S. (2004) Precipitation distribution tropical cyclones using the tropical rainfall measuring mission (TRMM) microwave imager: a global perspective. *Monthly Weather Review*, 132(7), 1645–1660. Available from: https://doi.org/10.1175/1520-0493(2004)132%3C1645:PDITCU%3E2.0.CO;2

Lonfat, M., Rogers, R., Marchok, T. & Marks, F.D., Jr. (2007) A parametric model for predicting hurricane rainfall. *Monthly Weather Review*, 135(9), 3086–3097. Available from: https://doi.org/10.1175/MWR3433.1

Marks, F. & DeMaria, M. (2003) *Development of a tropical cyclone rainfall climatology and persistence (R-CLIPER) model*. Technical report. NOAA/OAR/AOML/Hurricane Research Division.

Mühr, B., Daniell, J., Bessel, T., Brink, S. & Kunz, M. (2014) TYPHOON 09W "RAMMASUN" – short summary. In: *Center for Disaster Management and Risk Reduction Technology (CEDIM) forensic disaster analysis Group (FDA)*. Karlsruhe, Germany: Center for Disaster Management and Risk Reduction Technology, the Karlsruhe Institute of Technology.

Nguyen Van, T., Nguyen Dang, M., Mai Van, K., Trinh Hoang, D., Duong Van, K., Tran Thanh, T. et al. (2022) Climatic factors associated with heavy rainfall in northern Vietnam in boreal spring. *Advances in Meteorology*, 2022, 5917729. Available from: https://doi.org/10.1155/2022/5917729 14.

Osuri, K.K., Ankur, K., Nadimpalli, R. & Busireddy, N.K.R. (2020) Error characterization of ARW model in forecasting tropical cyclone rainfall over North Indian Ocean. *Journal of Hydrology*, 590, 125433. Available from: https://doi.org/10.1016/j.jhydrol.2020.125433

Paterson, L.A., Hanstrum, B.N., Davidson, N.E. & Weber, H.C. (2005) Influence of environmental vertical wind shear on the intensity of hurricane-strength tropical cyclones in the Australian region. *Monthly Weather Review*, 133(12), 3644–3660. Available from: https://doi.org/10.1175/MWR3041.1

Pham-Thanh, H., Ngo-Duc, T., Matsumoto, J., Phan-Van, T. & Vo-Van, H. (2020) Rainfall trends in Vietnam and their associations with tropical cyclones during 1979–2019. *Scientific Online Letters on the Atmosphere*, 16, 169–174. Available from: https://doi.org/10.2151/sola.2020-029

Rodgers, E.B., Adler, R.F. & Pierce, H.F. (2000) Contribution of tropical cyclones to the North Pacific climatological rainfall as observed from satellites. *Journal of Applied Meteorology and Climatology*, 39(10), 1658–1678. Available from: https://doi.org/10.1175/1520-0450(2000)039<1658:COTCTT>2.0.CO;2

Smith, R.B. & Barstad, I. (2004) A linear theory of orographic precipitation. *Journal of the Atmospheric Sciences*, 61(12), 1377–1391. Available from: https://doi.org/10.1175/1520-0469(2004)061<1377:ALTOOP>2.0.CO;2

Sun, C. & Liang, X.Z. (2020) Improving US extreme precipitation simulation: sensitivity to physics parameterizations. *Climate Dynamics*, 54(11), 4891–4918. Available from: https://doi.org/10.1007/s00382-020-05267-6

Wang, C., Liang, J. & Hodges, K.I. (2017) Projections of tropical cyclones affecting Vietnam under climate change: downscaled HadGEM2-ES using PRECIS 2.1. *Quarterly Journal of the Royal Meteorological Society*, 143(705), 1844–1859. Available from: https://doi.org/10.1002/qj.3046

Wells, M., Swinkels, R. & Turk, C. (2005) *Regional poverty assessment: red River Delta region*, Vol. 53. Washinton, D.C: World Bank Group, p. 2 Available at: http://documents.worldbank.org/curated/en/414651468315309898/Regional-poverty-assessment-Red-River-Delta-Region [Accessed 20 June 2022]

Willmott, C.J. (1981) On the validation of models. *Physical Geography*, 2(2), 184–194. Available from: https://doi.org/10.1080/02723646.1981.10642213

Wingo, M.T. & Cecil, D.J. (2010) Effects of vertical wind shear on tropical cyclone precipitation. *Monthly Weather Review*, 138(3), 645–662. Available from: https://doi.org/10.1175/2009MWR2921.1

Yu, Z., Wang, Y. & Xu, H. (2015) Observed rainfall asymmetry in tropical cyclones making landfall over China. *Journal of Applied Meteorology and Climatology*, 54(1), 117–136. Available from: https://doi.org/10.1175/JAMC-D-13-0359.1

Yu, Z., Wang, Y., Xu, H., Davidson, N., Chen, Y., Chen, Y. et al. (2017) On the relationship between intensity and rainfall distribution in tropical cyclones making landfall over China. *Journal of Applied Meteorology and Climatology*, 56(10), 2883–2901. Available from: https://doi.org/10.1175/JAMC-D-16-0334.1

Yu, Z., Wang, Y., Yu, H. & Duan, Y. (2022) The relationship between the inner-Core size and the rainfall distribution in Landfalling tropical cyclones over China. *Geophysical Research Letters*, 49(8), e2021GL097576. Available from: https://doi.org/10.1029/2021GL097576

How to cite this article: Angkanasirikul, W., Jian, W., & Lo, E. Y.-M. (2024). An asymmetric tropical cyclone rainfall model in the Northern Vietnam coast. *Meteorological Applications*, *31*(5), e70004. https://doi.org/10.1002/met.70004

APPENDIX A

There are seven metrics used to quantify the performance the of the parametric rainfall model in reproducing the TC-induced rainfall within the 500-km radial distance from the TC center. These metrics are examined in three levels: domain-, quadrant-, and grid-level analysis. In the quadrant-level analysis, the error between observation and prediction is quantified using the root-mean-square error (RMSE), the normalized RMSE (NRMSE), and the bias of an estimator (Bias), while for the domain-level analysis, the RMSE and Bias are used.

$$\mathrm{RMSE} = \sqrt{\frac{1}{n}\sum_{i=1}^{n}(y_i - x_i)^2} \tag{A1}$$

$$\mathrm{NRMSE} = \sqrt{\frac{\sum_{i=1}^{n}(y_i - x_i)^2}{n(x_{max} - x_{min})^2}} = \frac{\mathrm{RMSE}}{x_{max} - x_{min}} \tag{A2}$$

$$\mathrm{Bias} = \frac{1}{n}\sum_{i=1}^{n}(x_i - y_i) \tag{A3}$$

here x and y are the observation and prediction, respectively, and n is the data size. x_{min} and x_{max} are the minimum and maximum of the observation, respectively. The Willmott score skill (Skill) (Willmott, 1981) is calculated as

$$\mathrm{Skill}\,(X,Y) = 1 - \frac{\sum_{i=1}^{n}(y_i - x_i)^2}{\sum_{i=1}^{n}(|y_i - \bar{x}| + |x_i - \bar{x}|)^2} \tag{A4}$$

where $\bar{x}$ is the average value of the observation. A skill value of 1 indicates the perfect agreement.

In the microscale analysis, the Pearson coefficient correlation (PCC) is calculated as

$$\mathrm{PCC} = \frac{n\sum_{i=1}^{n}x_i y_i - \sum_{i=1}^{n}x_i \sum_{i=1}^{n}y_i}{\sqrt{\left[n\sum_{i=1}^{n}x_i^2 - \left(\sum_{i=1}^{n}x_i\right)^2\right]\left[n\sum_{i=1}^{n}y_i^2 - \left(\sum_{i=1}^{n}y_i\right)^2\right]}} \tag{A5}$$

The threat score (TS) and equitable threat score (ETS) are computed as follows:

$$\mathrm{TS} = \frac{\mathrm{Hits}}{\mathrm{Hits} + \mathrm{Misses} + \mathrm{False\ alarms}} \tag{A6}$$

where.

		Observed rainfall intensity	
		Above threshold	**Below threshold**
Forecasted rainfall intensity	Above threshold	Hit	False alarm
	Below threshold	Miss	Correct rejection

The ETS is computed as

$$\mathrm{ETS} = \frac{\mathrm{Hits} - \mathrm{Hits\ expected\ by\ chance}}{\mathrm{Hits} + \mathrm{Misses} + \mathrm{False\ alarms} - \mathrm{Hits\ expected\ by\ chance}} \tag{A7}$$

where.

Hits expected by chance

$$= \frac{(\mathrm{Hits} + \mathrm{False\ alarms}) \times (\mathrm{Hits} + \mathrm{Misses})}{(\mathrm{Hits} + \mathrm{False\ alarms} + \mathrm{Misses} + \mathrm{Correct\ rejections})} \tag{A8}$$